

The Influence of a Heat Source Position Located on the Bottom Wall Inside Square Enclosure on Laminar Natural Convection

Ihsan Ali Ghani
Mechanical Engineering Departement
College of Engineering
Almustansiriya University

Abstract

Natural convection in two-dimensional square enclosure is studied numerically using a finite difference method. In the present study, top wall is considered adiabatic, two vertical walls are maintained at constant low temperature, the bottom wall is maintained at constant high temperature and the non-heated parts of the bottom wall are considered adiabatic. The aim of this work is to determine the influence of the position of a small heating source located on the bottom wall of a square enclosure (aspect ratio=1) filled with air ($Pr=0.71$) on the natural convection flow. Three different positions are analyzed, on the left side ($\delta=0.1$), on the center ($\delta=0.5$) and on the right side ($\delta=0.9$). The dimensionless of the heat source length (S) is taken equal to (0.2). The three dimensional differential conservation equations of mass, momentum and energy are solved by a finite difference method for Rayleigh number varying from 10^3 to 10^6 . Results are presented in the form of streamline and isotherm plots as well as the variation of the Nusselt number at the heat source surface under different conditions. The average Nusselt number and flow behavior are symmetrical for both cases, when heat source located on the left extreme and right extreme of the bottom wall. The average Nusselt number for the extremes (left and right) is higher than the central position for ($Ra \leq 10^5$) because the heat source is adjacent to the cold vertical wall. The average Nusselt number for the central position is higher than the extremes (left and right) for ($Ra > 10^5$) because the vortexes rotation of the air in the center of the bottom wall is greater than extremes. The local Nusselt number is very high at the edges of the heat source and reduces towards the center.

Keywords: Natural convection, rectangular enclosure, finite difference method, Nusselt number.

الخلاصة

اجريت دراسته عدديه لانتقال الحرارة بالحمل الحر في حيز مربع باستخدام طريقة الفروقات المحدده. ان الحيز في وضع عمودي وقد تم ابقاء الجدران العموديان للحيز على درجه حراره منخفضه وكذلك تم عزل الجدار العلوي اما بالنسبه للجدار السفلي فقد تم تسخينه جزئيا بواسطة مصدر حراري في درجه حراره عاليه اما الجزء المتبقي من الجدار فقد تم عزله. ان الهدف من البحث هو دراسة تأثير موقع المصدر الحراري في الجدار السفلي على انتقال الحرارة بالحمل الحر للحيز المربع المملؤ بالهواء ($Pr=0.7$) وذلك باعتماد ثلاثة مواقع هي اقصى اليسار ($\delta=0.1$) وفي المنتصف ($\delta=0.5$) واقصى اليمين ($\delta=0.9$). وقد تم حل المعادلات التفاضليه ذات البعدين الخاصه بحفظ ماده والطاقه والزخم باستخدام طريقة الفروقات المحدده لعدة قيم لرقم رالي بين (10^3 - 10^6) وقد درست التغيرات في درجه الحراره وحقول السريران مع زيادة رقم رالي للمواقع المذكورة. وقد وجد في الدرسته انه عندما يوضع المصدر الحراري على طرفي الجدار السفلي (اليمين واليسار) فان معدل رقم نسلت وسلوك الجريان سيكونان متماثلان وذلك لتمائل الشكل الهندسي والظروف الحديه وقد وجد ايضا ان قيم معدل رقم نسلت اعلى في حالة كون المصدر الحراري على الاطراف (اليمين واليسار) مما هو عليه عندما يكون في وسط الجدار لقيم عدد رالي اصغر من او يساوي (10^5) وذلك نتيجة لتأثير الجدران العموديه الباردة الملاصقه للمصدر الحراري وكانت قيم معدل رقم نسلت في وسط الجدار اعلى منه عند الاطراف لقيم عدد رالي اكبر من (10^5) وذلك لأن السرعة الدواميه في وسط الحيز ستزداد وتؤدي الى زيادة انتقال الحرارة.

Nomenclature

C_p	specific heat at constant pressure, Ws/K kg
Gr	Grashof number
g	gravitational acceleration, m/s ²
h	heat transfer coefficient, W/m ² K
k	thermal conductivity, W/m K
L	enclosure width = enclosure height, m
Nu	local Nusselt number = hL/k
Pr	Prandtl number, $cp \mu/k$
Ra	Rayleigh number = $Gr.Pr$
S	heater length, m
T	temperature, K
u,v	velocity components in the x and y direction, m/s
U,V	dimensionless velocity components
x,y	space coordinates in cartesian system
X,Y	dimensionless cartesian coordinates

Greek Symbols

β	Coefficient of volumetric thermal expansion, K. ⁻¹
δ	dimensionless position of the heat source
θ	dimensionless temperature
μ	dynamic viscosity, kg/ms
ν	kinematic viscosity, m ² /s
ρ	density kg /m ³
ψ	non-dimensional stream function
ω	non-dimensional vorticity

Subscripts

c	cold surface
h	hot surface

INTRODUCTION

Natural convection in a closed square cavity has occupied the center stage in many fundamental heat transfer analysis which is of prime importance in certain technological applications. In fact, buoyancy-driven convection in a sealed cavity with differentially heated isothermal walls is a prototype of many industrial application such as operation and safety of nuclear reactors, convective heat transfer associated with boilers, solar energy system, cooling of the electronic circuits [1], ventilation of buildings[2] ,solar ponds and solar collectors[3,4,5].

The importance of free convection heat transfer phenomena taking place in enclosures is recognized by the abundant research works reviewed by Ostrach[6] and Yang[7]. Two dimensional natural convection in a differentially heated square enclosure has been solved numerically by de Vahl Davis[8], Markatos[9] and Barakos[10], their solutions agree well for the region of laminar flow, $Ra \leq 10^6$.

However, in most of these studies, one vertical wall of the enclosure is cooled and another one heated while the remaining top and bottom walls are well insulated. November and Nansteel [11] and Valencia and Frederick [12] have shown a specific interest to focus on a natural convection within a rectangular enclosure where in a bottom heating and/or a top cooling are involved. Studies on natural convection in rectangular enclosures heated from below and cooled along a single side or both sides have been carried out by Ganzarolli and Milanez [13]. Later, the case of heating from one side and cooling from the top has been analyzed by Aydin et al. [14] who investigated the influence of aspect ratio for air-filled rectangular enclosures. Also, Kirkpatrick and Bohn [15] examined experimentally the case of high Rayleigh number natural convection in a water-filled cubical enclosure heated simultaneously from below and from the side. Recently, Corcione [16] has studied natural convection in an air-filled rectangular enclosure heated from below and cooled from above for a variety of thermal boundary conditions at the side walls. Numerical results were reported for several values of both width-to-height aspect ratio of the enclosure and Rayleigh number.

Aydin et al. [17] simulated numerically the natural convective heat transfer of air in a square cavity cooled from the side walls and heated by a strip placed at the center of the bottom wall. Nibarufata et al. [18] analyzed numerically the natural convection in partitioned enclosures with a localized heating from below. Ramos and Milanez's [19] treated the natural convection in cavities heated from below by a thermal source, which dissipated energy at a constant rate.

The aim of this work is to determinate the influence of the position of a small heating source located in the bottom of a square cavity filled with air ($Pr=0.71$) on the natural convection heat transfer and fluid circulation. Three different positions are analyzed , on the left side of the bottom wall ($\delta=0.1$) , on the center ($\delta=0.5$) and on the right ($\delta=0.9$).

The length of the heat source (S) is taken equal to(0.2) for Rayleigh number varying from(10^3) to (10^6) and for the case when top wall is considered adiabatic, two vertical walls are maintained at constant low temperature, the heating source which located on the bottom wall is maintained at constant high temperature and the non-heated parts of the bottom wall are considered adiabatic.

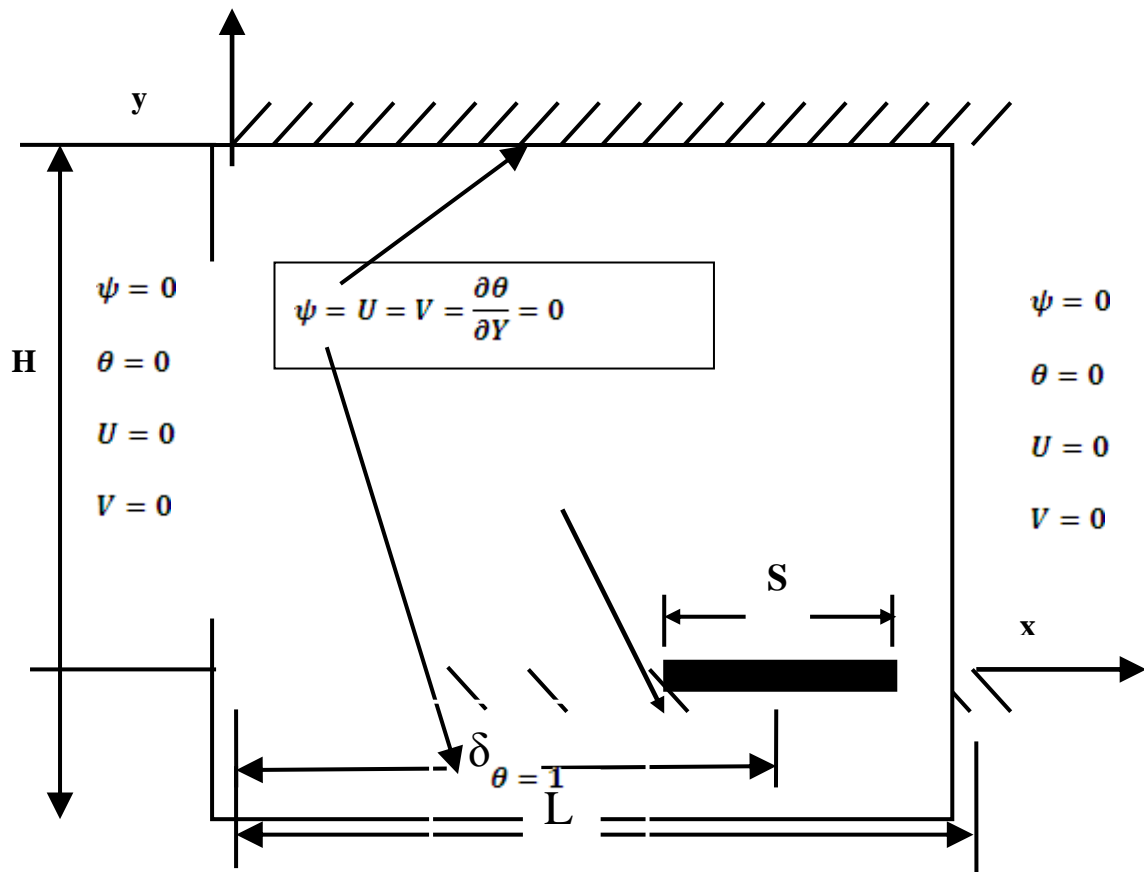


Fig.(1) Schematic of enclosure configuration

1. Mathematical Model

The configuration of interest for the present study is shown in figure (1). Two dimensional square enclosure with side of length (L) and adiabatic top wall. The left and right vertical walls maintained at constant low temperature. The bottom wall has a flush strip heater of constant temperature, which is located on three different locations , at ($\delta=0.1$), ($\delta=0.5$) and ($\delta=0.9$) which measured from the origin as shown in fig.(1)

Natural convection is governed by the differential equations expressing conservation of mass, momentum and energy. The present flow is considered unsteady, laminar, incompressible and two-dimensional. The viscous dissipation term in the energy equation is neglected.

The Boussinesq approximation is invoked for the fluid properties to relate density changes to temperature changes, and to couple in this way the temperature field to the flow

field. Then the governing equations for unsteady natural convection can be expressed in form as:

$$\frac{\partial u}{\partial x} + \frac{\partial v}{\partial y} = 0 \tag{1}$$

$$\frac{\partial u}{\partial t} + u \frac{\partial u}{\partial x} + v \frac{\partial u}{\partial y} = -\frac{1}{\rho} \frac{\partial p}{\partial x} + \nu \left[\frac{\partial^2 u}{\partial x^2} + \frac{\partial^2 u}{\partial y^2} \right] \tag{2}$$

$$\frac{\partial v}{\partial t} + u \frac{\partial v}{\partial x} + v \frac{\partial v}{\partial y} = -\frac{1}{\rho} \frac{\partial p}{\partial y} + \nu \left[\frac{\partial^2 v}{\partial x^2} + \frac{\partial^2 v}{\partial y^2} \right] + g\beta(T - T_C) \tag{3}$$

$$\frac{\partial T}{\partial t} + u \frac{\partial T}{\partial x} + v \frac{\partial T}{\partial y} = \alpha \left[\frac{\partial^2 T}{\partial x^2} + \frac{\partial^2 T}{\partial y^2} \right] \tag{4}$$

With boundary conditions:

$$u(x,0) = u(x,H) = u(0,y) = u(L,y) = 0$$

$$v(x,0) = v(x,H) = v(0,y) = v(L,y) = 0$$

$$\frac{\partial T}{\partial y} = 0 \rightarrow 0 < x < \delta - \frac{S}{2} \quad \text{and} \quad \delta + \frac{S}{2} < x < L$$

$$T = T_H \rightarrow \delta - \frac{S}{2} < x < \delta + \frac{S}{2}$$

Where (x) and (y) are the distances measured along the horizontal and vertical directions, respectively; (u) and (v) are the velocity components in the \mathbf{x} - and \mathbf{y} -directions, respectively; (T) denotes the temperature; (ν) and (α) are kinematic viscosity and thermal diffusivity, respectively; (p) is the pressure and (ρ) is the density; (T_H) and (T_C) are the temperatures at hot bottom wall and cold vertical walls, respectively; (L) is the width of the enclosure ; (S) is the length of the heat source ; (δ) is the horizontal distance from origin to center of the heated strip.

Using the following dimensionless parameters according to ref.[18] :

$$X = \frac{x}{H} , \quad Y = \frac{y}{H} , \quad U = H \frac{u}{\alpha} , \quad V = H \frac{v}{\alpha} , \quad P = \frac{pH^2}{\rho\alpha^2} , \quad \tau = \alpha \frac{t}{H^2}$$

$$\theta = \frac{T - T_\infty}{T_w - T_\infty} , \quad Gr = \frac{g\beta(T_w - T_\infty)H^3}{\nu^2} , \quad Ra = Gr.Pr$$

the governing equations (1)–(4) reduce to non-dimensional form:

$$\frac{\partial U}{\partial X} + \frac{\partial V}{\partial Y} = 0 \tag{5}$$

$$\frac{\partial U}{\partial \tau} + U \frac{\partial U}{\partial X} + V \frac{\partial U}{\partial Y} = -\frac{\partial P}{\partial X} + Pr \left[\frac{\partial^2 U}{\partial X^2} + \frac{\partial^2 U}{\partial Y^2} \right] \tag{6}$$

$$\frac{\partial V}{\partial \tau} + U \frac{\partial V}{\partial X} + V \frac{\partial V}{\partial Y} = -\frac{\partial P}{\partial Y} + \text{Pr} \left[\frac{\partial^2 V}{\partial X^2} + \frac{\partial^2 V}{\partial Y^2} \right] + \text{Ra.Pr.}\theta \quad (7)$$

$$\frac{\partial \theta}{\partial \tau} + U \frac{\partial \theta}{\partial X} + V \frac{\partial \theta}{\partial Y} = \frac{\partial^2 \theta}{\partial X^2} + \frac{\partial^2 \theta}{\partial Y^2} \quad (8)$$

Eliminating the pressure gradient terms in Eqs. (6) and (7) by cross partial differentiation and introducing the vorticity function:

$$\omega = \frac{\partial V}{\partial X} - \frac{\partial U}{\partial Y} \quad (9)$$

The equation of vorticity will be:

$$\frac{\partial \omega}{\partial \tau} + \frac{\partial(U\omega)}{\partial X} + \frac{\partial(V\omega)}{\partial Y} = \text{Pr} \left[\frac{\partial^2 \omega}{\partial X^2} + \frac{\partial^2 \omega}{\partial Y^2} \right] + \text{Gr.Pr.} \frac{\partial \theta}{\partial X} \quad (10)$$

And the equation of energy will be:

$$\frac{\partial \theta}{\partial \tau} + \frac{\partial(U\theta)}{\partial X} + \frac{\partial(V\theta)}{\partial Y} = \frac{\partial^2 \theta}{\partial X^2} + \frac{\partial^2 \theta}{\partial Y^2} \quad (11)$$

By using the definition of stream function:

$$V = -\frac{\partial \psi}{\partial X} \quad (12)$$

and

$$U = \frac{\partial \psi}{\partial Y} \quad (13)$$

The equation of vorticity will be:

$$-\omega = \frac{\partial^2 \psi}{\partial X^2} + \frac{\partial^2 \psi}{\partial Y^2} \quad (14)$$

The boundary condition will be

$$\frac{\partial \theta}{\partial Y} = 0 \rightarrow 0 < X < \delta - \frac{s}{2} \quad \text{and} \quad \delta + \frac{s}{2} < X \leq L \quad (\text{nonheated parts of the bottom wall})$$

$$\frac{\partial \theta}{\partial Y} = 0 \rightarrow Y = H \quad \text{and} \quad 0 < X \leq L \quad (\text{Top wall})$$

$$\theta = 1 \rightarrow \delta - \frac{s}{2} < X < \delta + \frac{s}{2} \quad (\text{Heating source})$$

$$U = V = \psi = 0 \rightarrow X = 0 \quad \text{and} \quad 0 < Y < H \quad (\text{Left vertical wall})$$

$$U = V = \psi = 0 \rightarrow Y = 0 \quad \text{and} \quad 0 < X < L \quad (\text{Bottom wall})$$

$$U = V = \psi = 0 \rightarrow X = L \quad \text{and} \quad 0 < Y < H \quad (\text{Right vertical wall})$$

$$U = V = \psi = 0 \rightarrow Y = H \text{ and } 0 < X < L \quad (\text{Top wall})$$

$$\omega = -\frac{\partial^2 \psi}{\partial Y^2} \quad (\text{At the bottom wall})$$

by series expansions for stream function on the bottom wall the boundary vorticity will be:

$$\omega|_{i,0} = \frac{(-8\psi|_{i,1} + \psi|_{i,2})}{2(\Delta Y)^2}$$

Numerical solution

The equations are solved numerically using finite difference method with a regular Cartesian space grid. Suppose that all quantities $(\theta_{i,j,n}, \omega_{i,j,n}, \psi_{i,j}^n)$ are known at time $(n\Delta t)$ to find the temperature and vorticity values at the interior grid points in the next time level $(n+1)\Delta t$. For this, forward difference approximation is used for time derivative and central difference approximations are used for all spatial derivatives. The method of successive over relaxation (SOR) is then used in conjunction with the newly computed temperatures $(\theta_{i,j,n+1})$ and vorticities $(\omega_{i,j,n+1})$ to solve the stream function equation for the new improved stream function $(\psi_{i,j}^{n+1})$. After finding the stream function, the values of (U) and (V) at the current time level are computed using the central difference approximations to

$$U = \frac{\partial \psi}{\partial Y}$$

And

$$V = -\frac{\partial \psi}{\partial X}$$

This procedure is repeated at each time step. The boundary vorticities at the solid walls can be derived considering Taylor's series expansions for stream function in the vicinity of the walls. This computational cycle is repeated till steady state solution is obtained, that is, when the following convergence criteria:

$$|\phi_{i,j,n} - \phi_{i,j,n+1}| < 10^{-3}$$

for temperature, vorticity and stream function is met

Evaluation of Nusselt number

The local heat transfer rate along the heated section of the wall is obtained from the heat balance that gives an expression for the local Nusselt number as:

$$Nu = -\frac{\partial \theta}{\partial Y}|_{Y=0}, \quad X_1 < X < X_2$$

Where $X_1 = \delta - \frac{s}{2}$, $X_2 = \delta + \frac{s}{2}$

The average value for Nusselt number is defined by:

$$Nu = \frac{1}{X_2 - X_1} \int_{X_1}^{X_2} - \frac{\partial \theta}{\partial Y} \Big|_{Y=0} dX$$

four different grid densities 21 × 21, 31 × 31, 41 × 41 and 51×51. The minimum value of the stream function of the primary vortex (ψ_{min}) is commonly used as a sensitivity measure of the accuracy of the solution. Quantity (ψ_{min}) is selected as the monitoring variable for the grid independence study. Comparison of (ψ_{min}) values among four different cases suggests that the two grid distributions 41×41 and 51 × 51 gives nearly identical results. Considering both the accuracy and the computational time, the following calculations were all performed with a 41×41 grid.

Results and Discussion

The working fluid is chosen as air with Prandtl number, Pr = 0.71. The normalized length of the constant heat source at the bottom wall(S) is taken to (0.2) and the Rayleigh number (Ra) is varied from (10³) to (10⁶) .In order to validate the numerical model, the results are compared with those reported by Aydin and Yang[17], for (Ra = 10³ to 10⁶) ,(S = 0.2). In figure (2), a comparison of the average Nusselt number of the heat source located in the middle of the bottom wall is presented. The agreement is found to be acceptable which validates the present computations indirectly.

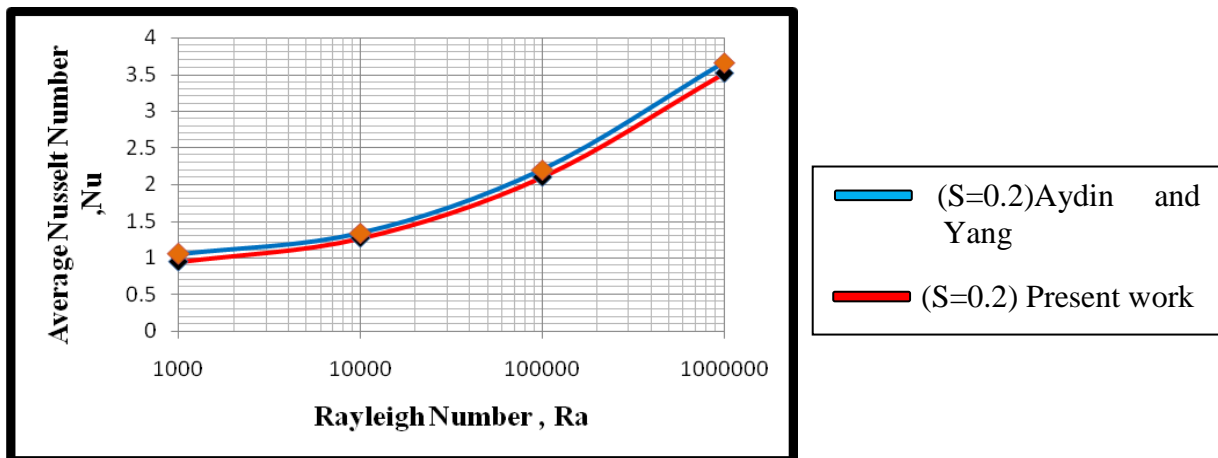


Fig.(2) Comparison between present work and Aydin – Yang[17] when the heating source located on the center position of the bottom wall

1. Effect of Rayleigh Numbers:

1.1. Heating source in the center of the bottom wall (δ= 0.5):

The evolution of the flow and thermal fields with Rayleigh number for an enclosure of a representative case with dimensionless heat source length (S= 0.2) and (δ=0.5)is presented in Figures(3 to 6) . For various (Ra = 10³-10⁶), the flow pattern is characterized by two symmetrical rolls with clockwise and anti- clockwise rotations inside the enclosure.

The hot fluid rises in the central region as a result of buoyancy forces, and then it descends downwards along the vertical walls and turns horizontally to the central region after hitting the bottom wall. The flow then rises along the vertical symmetry axis and gets blocked at the adiabatic top wall, which turns the flow horizontally towards the cold vertical walls. Thus a pair of counter rotating circulation cells is formed in the flow domain.

At ($Ra = 10^3$), as can be expected, heat transfer from the discrete heat source is essentially dissipated via a conduction-dominated mechanism as indicated by the isotherm pattern shown in Fig.(3)

For ($Ra = 10^4$), the buoyant convection flow in the central region between the rolls distorts the isotherms field. The distortion of the isotherm field increases with enhanced buoyancy as (Ra) increases, where the heat transfer becomes increasingly convection dominated as seen in Fig.(4) the circulation near the central regimes are stronger and consequently, the temperature contour starts getting shifted towards the side wall and they break into two symmetric contour lines. The presence of significant convection is also exhibited in other temperature contours lines which start getting deformed and pushed towards the top wall.

As Rayleigh number increases to (10^5), the buoyancy driven circulation inside the cavity also increases as seen from Fig. (5). The circulations are faster near the center and slower near the wall due to no slip boundary conditions. The faster circulation in each half of the cavity follows a progressive wrapping around the centers of rotation, and a more pronounced compression of the isotherms toward the boundary surfaces of the enclosures occur. Consequently, at $Ra = 10^5$, the temperature gradients near both the bottom and side walls tend to be significant leading to the development of a thermal boundary layer. Due to greater circulations near the central core at the top half of the enclosure, there are small gradients in temperature whereas a large stratification zone of temperature is observed at the vertical symmetry line due to stagnation of flow.

With increase of (Ra) to (10^6) a transformation from a primarily two symmetrical rolls pattern to a structure characterized by two large vortices near the central regions, moving towards upper wall. Therefore, the prevailing conductive heat transfer for ($Ra= 10^3$) and the mushroom profile of the isotherms for ($Ra = 10^6$) are presented in Fig. (6). Also viscous forces are more dominant than the buoyancy forces at lower (Ra). At higher (Ra) when the intensity of convection increases significantly, the core of the circulating rolls moves up and the isotherm patterns changes significantly indicating that the convection is the dominating heat transfer mechanism in the enclosure

1.2 Heating source in the left or right of the bottom wall ($\delta= 0.1$ and $\delta = 0.9$):

It is found that the results are symmetrical for both cases, when the heat source located on the left extreme position ($\delta = 0.1$) or on the right extreme position ($\delta = 0.9$) of the bottom wall.

At ($Ra = 10^3$), as can be expected, heat transfer from the discrete heat source is essentially dissipated via a conduction-dominated mechanism as indicated by the isotherm pattern shown in Fig. (7)(left) and Fig.(8)(right).

In the first case when the heat source is located in the center of the bottom wall two recirculation cell is formed and the solution is symmetric about the vertical midline due to the symmetry of the problem geometry and boundary conditions. When the heat source located in the left or in the right of enclosure this symmetry is completely destroyed when the left recirculating vortex(or right) becomes dominating in the enclosure while the right vortex(or left) is squeezed thinner and ultimately is divided into two minor corner vortices. This circulation inside the cavity is greater near the center and least at the wall due to no slip boundary conditions.

When (Ra) increases (10^4 - 10^6), the convection roll located at the left half of the square enclosure tends to merge in order to form a single large recirculation cell compared to two minor corner vortices. The isotherms are also adjusted according to the changes in the flow field and pushed towards the lower part of the right sidewall indicating the presence of a large temperature gradient there as shown in figures(9-14)

1.3. Heat transfer rates: local and average Nusselt numbers

Next attention is focused upon the influence of discrete heat source location on the heat transfer rate across the discretely heated enclosure .The variation of the average Nusselt number, Nu , at the heated surface with Rayleigh number, Ra , for the entire of the heated surface length (S), is shown in Fig.(15)from which some interesting trends are observed.In general, the average Nusselt number remains invariant up to a certain value of Rayleigh number and then increases briskly with increasing Rayleigh number. For low Rayleigh number, the curves maintain a flat trend that means low temperature gradients but(Nu) increases rapidly with (Ra)especially for ($Ra > 10^4$)because when ($Ra \geq 10^4$), the buoyancy aids more and more in the heat transfer process which results in more rapid increase of (Nu).

In fig.(15) its seen that the average Nusselt number for the case when the heating source located on the extremes (left and right) is greater than the average Nusselt number when the heating

Source located on the center of the bottom wall for the ranges of Rayleigh number ($10^3 < Ra < 10^5$) because the heating source is adjacent to the cold vertical wall (left and right) and that cause more heat transfer because the hot fluid loses part of its energy to the cold section of the vertical wall, but when the ($Ra = 10^6$) the Nusselt number for the center location ($Nu = 3.514$) is more than left and right ($Nu = 3.413$) (as seen in table (1)) because as (Ra) increase the two symmetrical vortices rotation increase the velocity of the air near heater strip this circulation inside the cavity is greater near the center and least at the wall.

Fig.(16) shows the effects of (Ra) on the local Nusselt numbers at the bottom wall. The local Nusselt number (Nu) is very high at the edges of the heat source due to the discontinuities present in the temperature boundary conditions at the edges and reduces towards the center of the heat source with the minimum value at the center and also due to the symmetrical boundary conditions, two symmetric convection cells are generated and their interface behaves like an insulator. The centre of the heat source surface becomes the stagnation point of the heat transfer area, and attains the maximum temperature and minimum heat transfer rate.

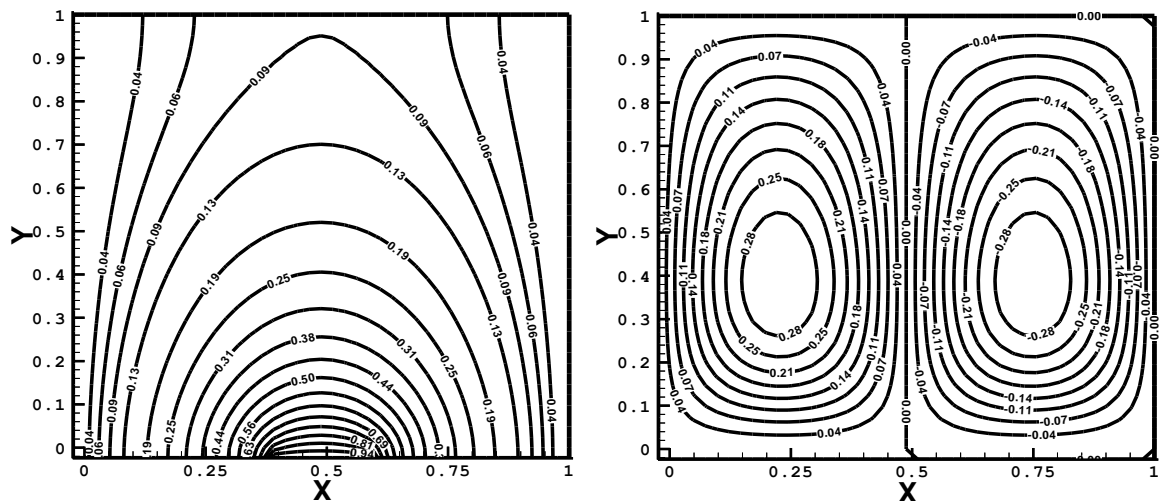


Fig. (3) Contour plots of isotherms and stream line for($Ra=10^3$)when heating source located on the center of the bottom wall

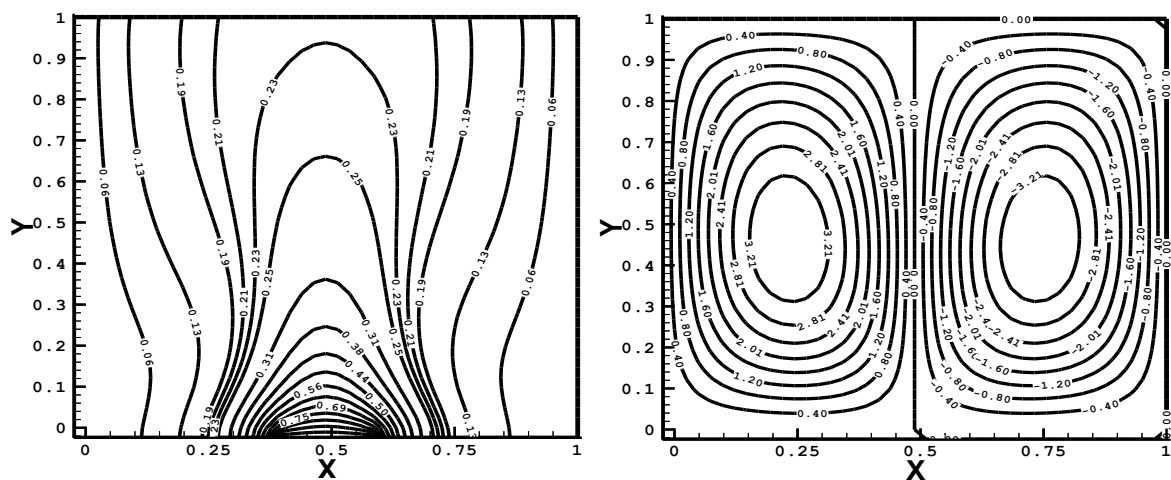


Fig. (4) Contour plots of isotherms and stream lines for($Ra=10^4$)when heating source located on the center of the bottom wall

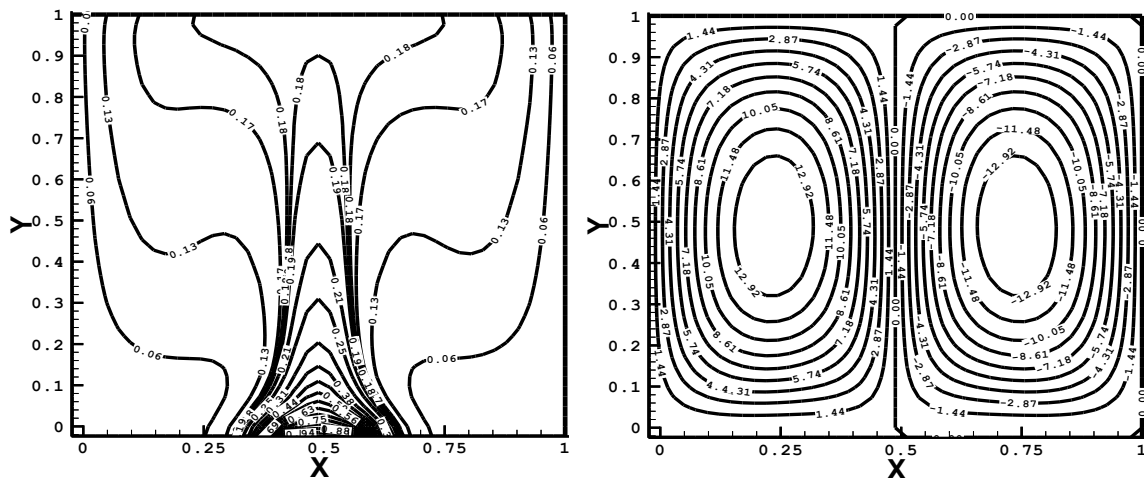


Fig. (5) Contour plots of isotherms and stream lines for ($Ra=10^5$) when heating source located in the center of the bottom wall

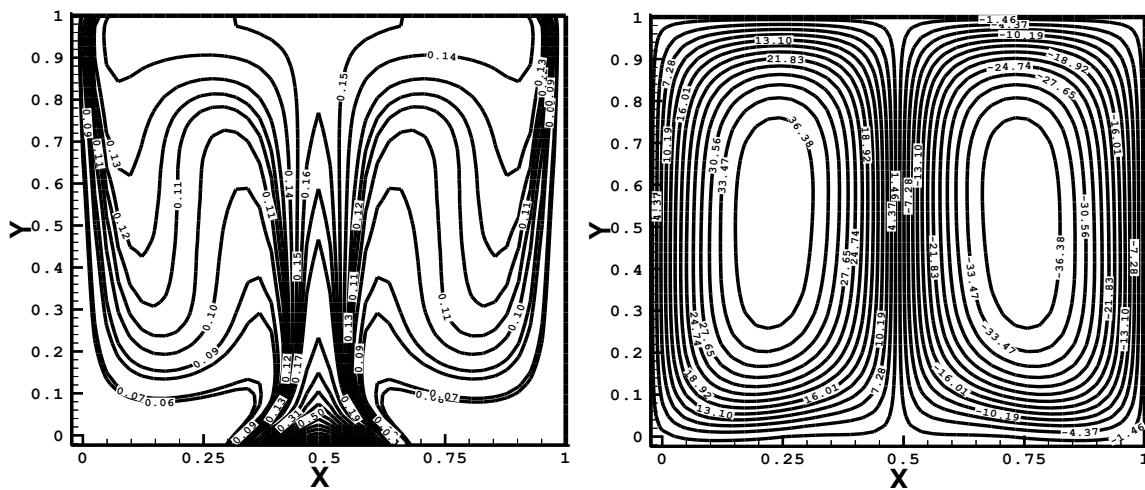


Fig. (6) Contour plots of isotherms and stream lines for ($Ra=10^6$) when heating source located on the center of the bottom wall

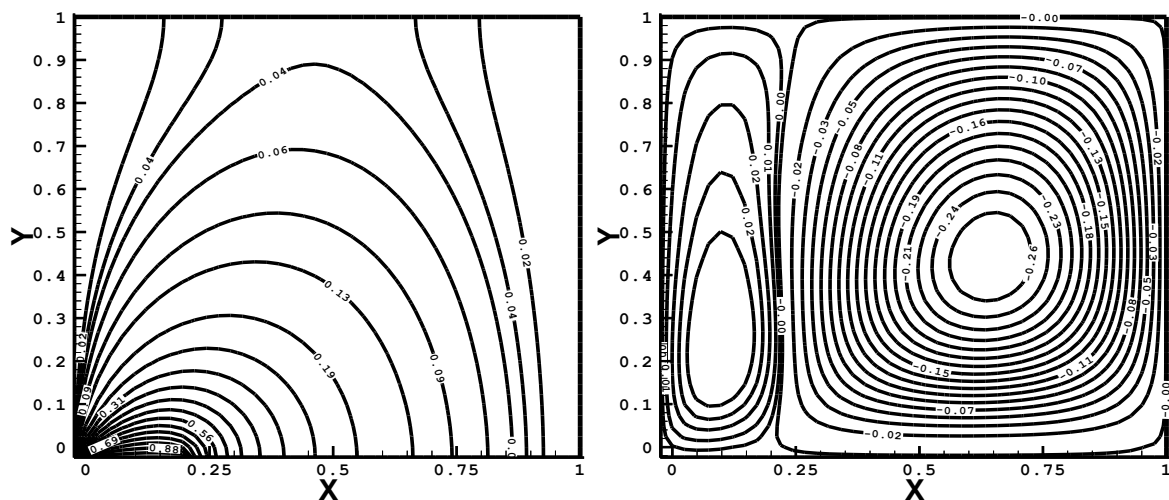


Fig. (7) Contour plots of isotherms and stream lines for ($Ra=10^3$) when heating source located on the left extreme of the bottom wall

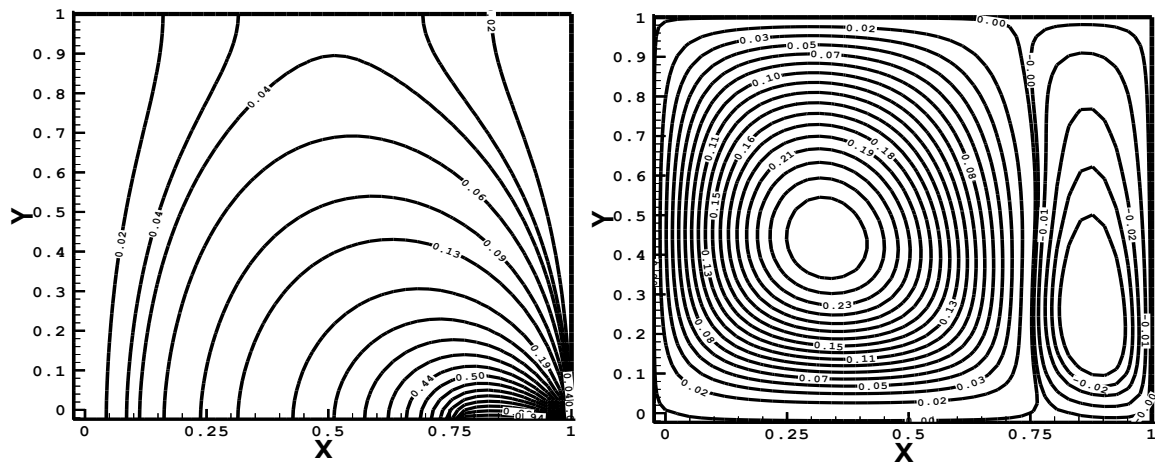


Fig. (8) Contour plots of isotherms and stream lines for ($Ra=10^3$) when heating source located on the right extreme of the bottom wall

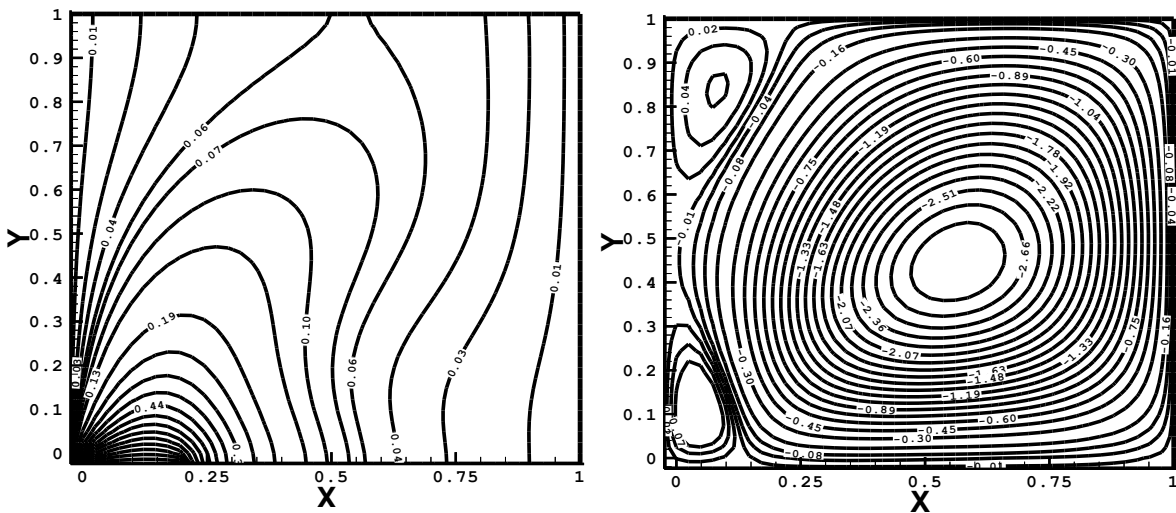


Fig. (9) Contour plots of isotherms and stream lines for ($Ra=10^4$) when heating source located on the left extreme of the bottom wall

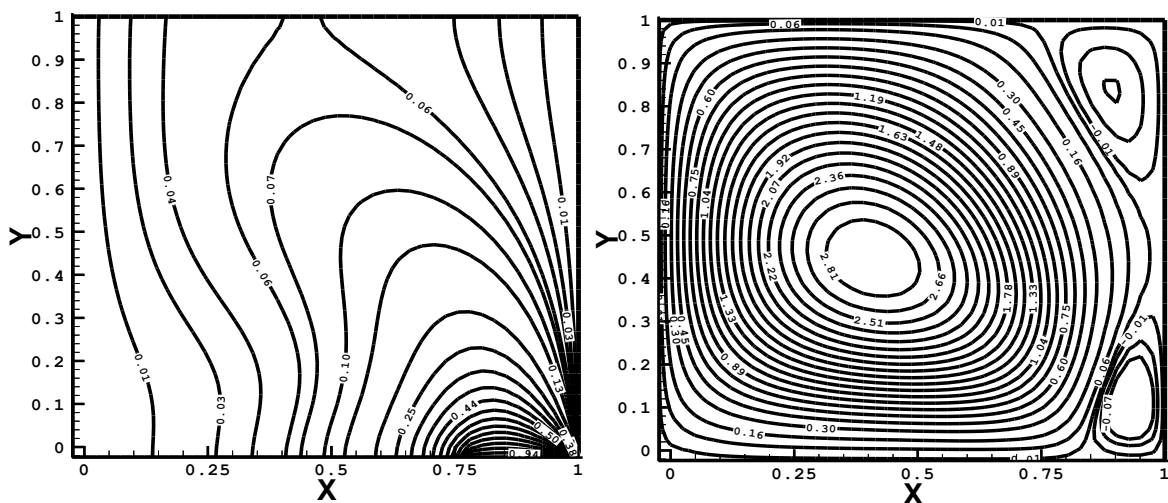


Fig. (10) Contour plots of isotherms and stream lines for ($Ra=10^4$) when heating source located on the right extreme of the bottom wall

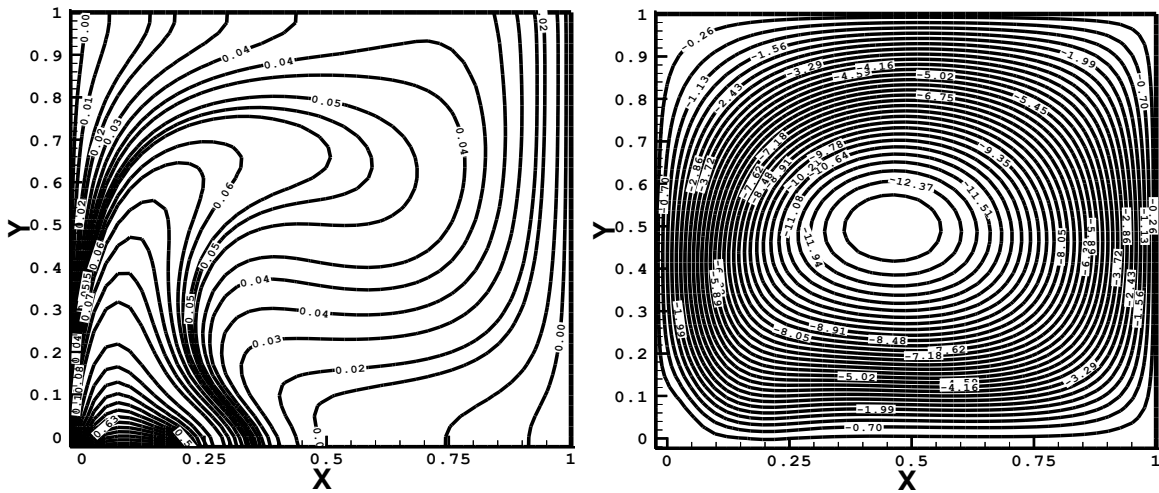


Fig. (11) Contour plots of isotherms and stream lines for ($Ra=10^5$) when heating source located on the left extreme of the bottom wall

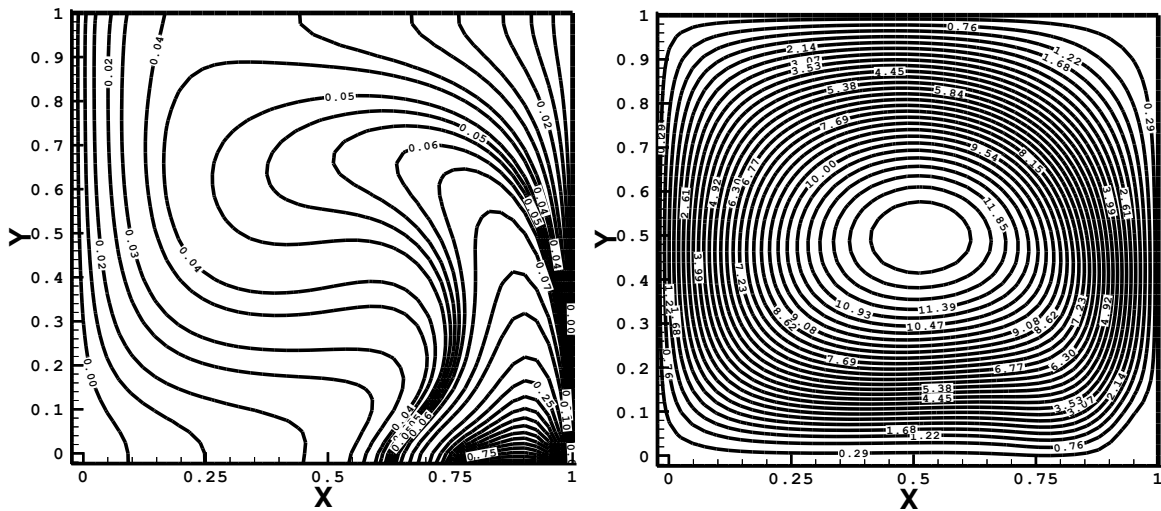


Fig. (12) Contour plots of isotherms and stream lines for ($Ra=10^5$) when heating source located on the right extreme of the bottom wall

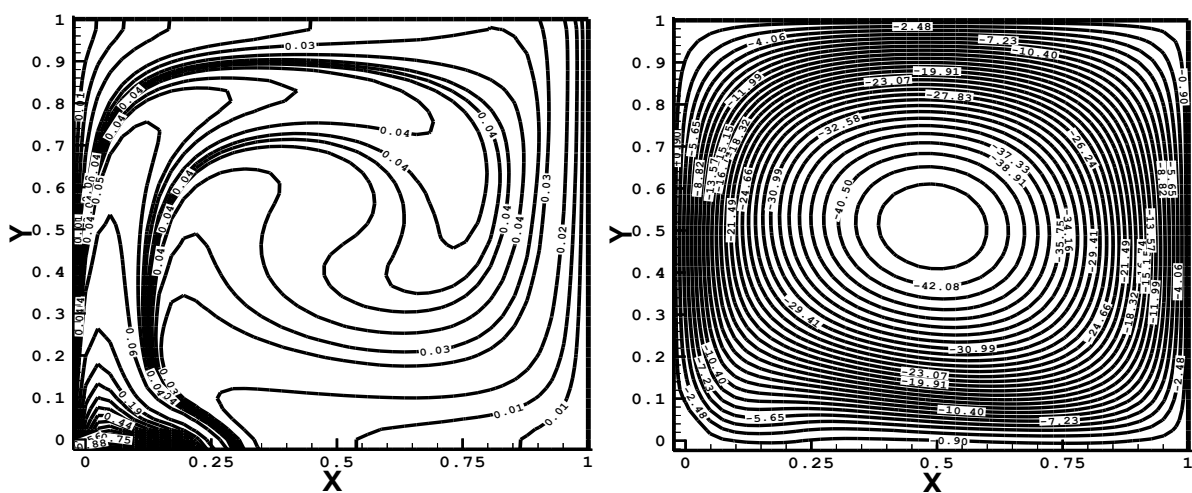


Fig. (13) Contour plots of isotherms and stream lines for ($Ra=10^6$) when heating source located on the left extreme of the bottom wall

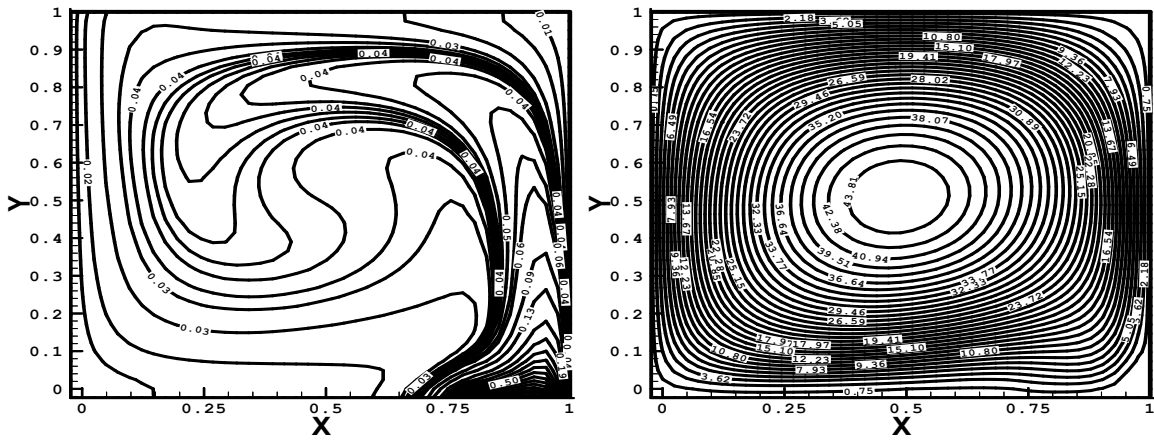


Fig. (14) Contour plots of isotherms and stream lines for $(Ra=10^6)$ when heating source located on the right extreme of the bottom wall

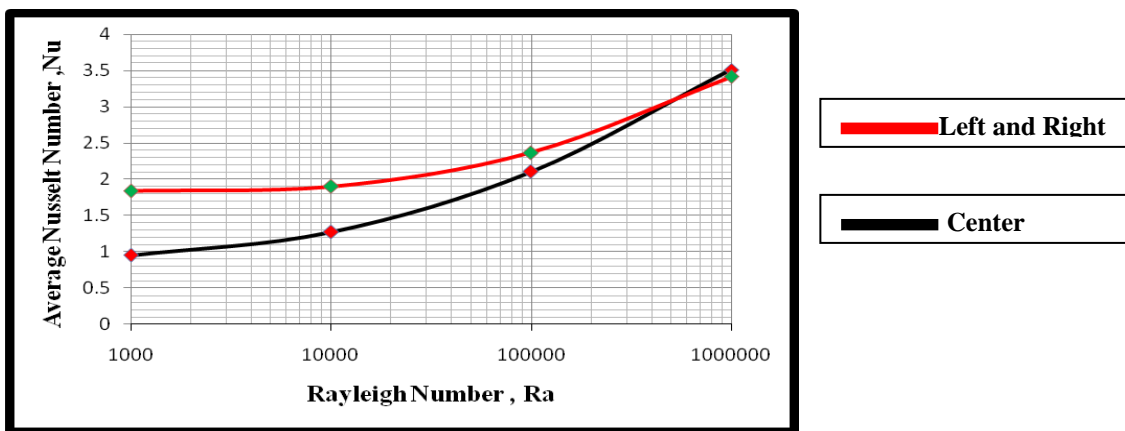


Fig. (15) Variation of average Nusselt number with Rayleigh number when heating source located on the extremes (left and right) and on the center of the bottom wall

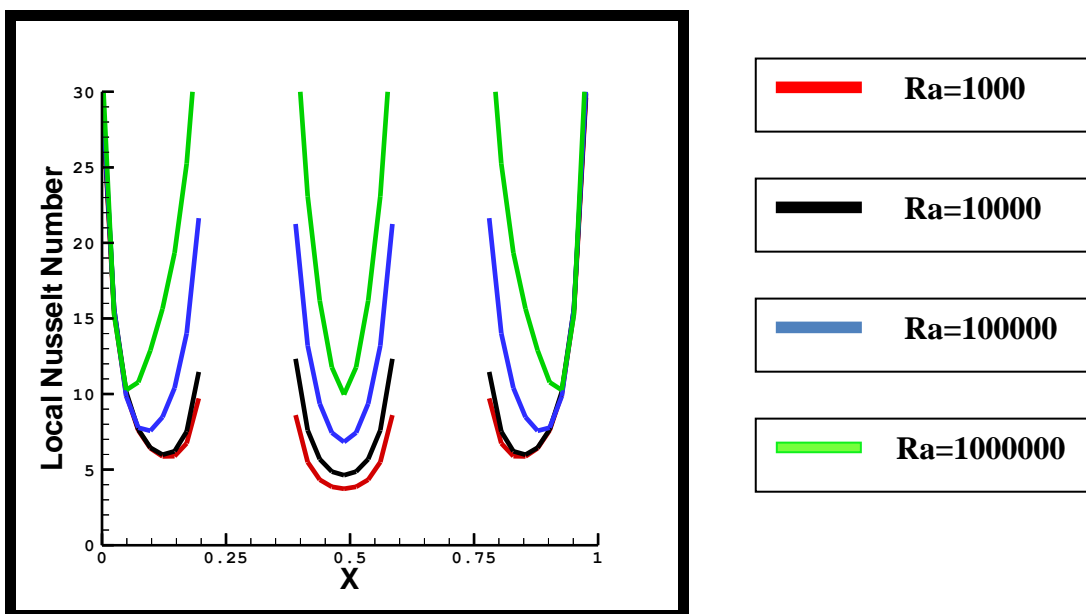


Fig. (16) Variation of local Nusselt number along the heating source surface (s) when located on the (left, center and right) sides of the bottom wall of the enclosure for Rayleigh numbers (10^3-10^6)

Table(1) the values of average Nusselt number for both cases ,when heating source located on the extremes(left and right) and when located on the center of the bottom wall

Rayleigh Number	Average Nusselt No./Center position	Average Nusselt No./left and right position
1000	0.9497	1.838
10000	1.272	1.903
100000	2.103	2.366
1000000	3.514	3.413

Conclusions

In this paper natural convection in an air filled square enclosure with a single flush discrete heater mounted on a bottom wall is studied. The enclosure consists of top adiabatic surface, two isothermal vertical walls and a flush isothermal hot strip located on the bottom wall. The partial differential equations for two dimensional conservation of mass, momentum and energy are solved based on central second order finite difference method. The solution scheme is validated by comparison with well established reference solutions. The model is then used to investigate the effect of hot strip location on both heat transfer and fluid flow patterns, within the cavity for fixed heater length ($s = 0.2$) and different positions, ($\delta = 0.1, 0.5$ and 0.9). From the results its found

- 1- When the heat source located on the left extreme position or on the right extreme position of the bottom wall, the average Nusselt number and flow behaviors are symmetrical because the geometry and the boundary conditions are symmetrical.
- 2- When ($Ra \leq 10^5$) the average Nusselt number for the extremes (left and right) are higher than that of central position .
- 3- When ($Ra > 10^5$) the average Nusselt number for the central position is higher than that for extremes (left and right).
- 4- The local Nusselt number is very high at the edges of the heat source and reduces towards the center .

References

1. **Incropera, F.P.**, Convection heat transfer in electronic equipment cooling, *ASME J. Heat Trans.* **110**, 1097-1111, (1988).
2. **Hoogendooren, G.J.** and **Afgan, N.H.** (Eds) *Energy Conservation in Heating, Cooling and Ventilating Buildings*, Hemisphere Pub. Washington D.C. (1978).
3. **Cha, C.K.** and **Jauria, Y.**, Recirculating Mixing Convection Flow for Energy Extraction, *Int. J. Heat Mass Transfer*, **27**, 1801-1810, (1984).
4. **Imberger, J.** and **Hamblin, P.F.**, Dynamics of Lakes, Reservoirs and Cooling Ponds, *A. Rev. Fluid Mech.*, **14**, 153-187, (1982).
5. **Ben Yedder, R., Du, Z.G.** and **Bilgen, E.**, Heat Transfer by Natural Convection in Composite Trombe Wall Solar Collector, *Proc. ASME, Solar Energy Technology, 1989, San Francisco*.
6. **Ostrach, S.**, Natural Convection in Enclosures, *Trans. ASME, J. Heat Transfer*, **110**, 1175-1190, (1988).
7. **Yang, K.T.**, Natural Convection in Enclosures, In, *Handbook of Single-Phase Convective Heat Transfer*, (Edited by **S. Kakac, R. Shah** and **W. Aung**) Wiley New York, Chap. 13, (1987).
8. **De Vahl Davis, G.**, Natural Convection of Air in a Square Cavity: A Benchmark Numerical Solution, *Int. J. Numerical Methods in Fluids*, **3**, 249-264, (1983).
9. **Markatos, N.C.** and **Pericleous, K.A.**, Laminar and Turbulent Natural Convection in an Enclosure Cavity, *Int. J. Heat Mass Transfer*, **27**, 5, 755-772, (1984).
10. **Barakos, G., Mitsoulis, E.** and **Assimacopoulos, D.**, Natural convection flow in a square cavity, revisited: Laminar and turbulent models with wall functions, *Int. J. for Numerical Methods in Fluids*, **18**, 695-719, (1994).
11. **M. November, M.W. Nansteel**, Natural convection in rectangular enclosures from below and cooled along one side, *Int. J. Heat Mass Transfer* **30** (1987) 2433–2440.
12. **A. Valencia, R.L. Frederick**, Heat transfer in square cavities with partially active vertically walls, *Int. J. Heat Mass Transfer* **32** (1989) 1567–1574.
13. **M.M. Ganzarolli, L.F. Milanez**, Natural convection in rectangular enclosures heated from below and symmetrically cooled from the sides, *Int. J. Heat Mass Transfer* **38** (1995) 1063–1073.
14. **O. Aydin, A. Unal, T. Ayhan**, Natural convection in rectangular enclosures heated from one side and cooled from the ceiling, *Int. J. Heat Mass Transfer* **5** (1999) 2345–2355.
15. **A.T. Kirkpatrick, M. Bohn**, An experimental investigation of mixed cavity natural convection in the high Rayleigh number regime, *Int. J. Heat Mass Transfer* **29** (1986) 69–82.
16. **M. Corcione**, Effects of the thermal boundary conditions at the sidewalls upon natural convection in rectangular enclosures heated from below and cooled from above, *Int. J. Therm. Sci.* **42** (2003) 199–208.

- 17. O. Aydin and W. J. Yang**, Natural convection in enclosures with localized heating from below and symmetrical cooling from sides, *Int. J. Num .Methods Heat Fluid Flow*, Vol.10, No. 5, 2000, pp. 519-529.
- 18. Tanmay Basak, S.Roy , A.R.Balakrishnan** Effect of thermal conditions on natural convection flows within a square cavity. *International of heat and mass transfer* 49.(2006) pp. 4525-4535
- 19. Nor Azwadi Che Sidik, Rosdzimin,A.R.M**, Simulation of Natural Convection Heat Transfer In An Enclosure Using Lattice Boltzmann Method.*Jurnal Mekanikal*,December 2008,No.27 42-50